*Tellus (2003), 55A, 181–191*
*Printed in UK. All rights reserved*


**TELLUS**
*ISSN 0280–6495*

# Spatial hierarchy in Arctic sea ice dynamics

By S. LYN MCNUTT[1] and JAMES E. OVERLAND[2]*, [1]*Geophysical Institute, University of Alaska, Fairbanks, Alaska, USA;* [2]*Pacific Marine Environmental Laboratory, NOAA, Seattle, Washington, USA*

(Manuscript received 11 October 2001; in final form 14 May 2002)

ABSTRACT

We define a new classification for Arctic sea ice dynamics based on a spatial and temporal scale: floe, multifloe, aggregate, coherent, sub-basin and seasonal. The classification is supported by remote sensing and in situ observations of ice motions at scales of 1–700 km, as found in the existing scientific literature. The first significant change in sea ice behavior appears as an "emergent" property of the sea ice at the transition from the multifloe scale (2–10 km/<1 d) to the aggregate scale (10–75 km/1–3 d). This emergent behavior establishes a statistical mechanical length where sea ice can be considered a plastic continuum. A second important, or coherent scale occurs at 75–300 km and 3–7 d, where the spatial/temporal processes of sea ice dynamics best match the scales of the wind forcing, i.e., winds of this duration and fetch are necessary to fully load the internal stress field. At scales smaller than the coherent scale, the spatial dimension is important because the sea ice motions on the coherent scale provide non-local forcing to the aggregate scale. At dimensions larger than the coherent scale, including the sub-basin and seasonal scales, spatial and temporal averaging occurs, which smooths discontinuities. To understand and model sea ice dynamics at each of these scales requires an understanding of the detail at the next smallest level. Proper understanding and representation of sea ice dynamics at all scales is critical to devising a sound strategy for data assimilation into sea ice models.

## 1. Introduction

Sea ice often appears self-similar across a range of geophysical scales. Low-altitude aerial photographs of Arctic sea ice are visually similar to high-altitude photographs and satellite imagery. Yet, there are discontinuities in sea ice dynamics due to both the internal structure of the ice pack and external forcing. Sea ice strength appears to decrease by three orders of magnitude as the scale increases from 1 m to 500 km (Sanderson, 1988). This suggests that different physics may be operating at different scales, or that some scale-dependent, self-similarity property is present. To understand and model sea ice dynamics, it is also important to know at what scales internal ice dynamics couple strongly with the predominant spatial and temporal scales of the external forcing, i.e., the windstress field.

*Corresponding author.
e-mail: overland@pmel.noaa.gov

Our purpose is to note a spatial hierarchy of sea ice dynamics based on recent evidence from remote sensing and in situ observations. Here we undertake an examination of sea ice dynamics based on recent literature, rather than through the introduction of new data. Improvements to present generation climate and regional sea ice models include higher spatial resolution, thereby necessitating a better, understanding definition, and incorporation of sea ice physics throughout a range of scales. Hierarchy theory itself is a useful method to classify sea ice dynamics (Overland et al., 1995; Goldenfeld and Kadanoff, 1999). Two concepts from hierarchy theory are important in establishing spatial and temporal length scales and interactions critical to understanding sea ice dynamics: emergent properties and coherent levels.

Our analysis also has implications for sampling strategies for observational data to initialize and validate sea ice models. We realize that internal stress data do not currently exist to fully test our classification and that many of our conclusions are inferred from ice motion data. However, we believe our synthesis provides a starting point for further discussions of real-world sea ice dynamics, modeling and data assimilation.

The first important concept from hierarchy theory is the notion of an emergent property (O'Neill et al., 1986). This property represents a scale discontinuity where the whole is greater than the sum of its parts. In biology, this is typically described as cells composing organs, or organs composing organisms. Here we argue for an emergent property of Arctic sea ice at the transition from the multifloe scale (2–10 km) to the aggregate scale (10–75 km). The emergent property of sea ice dynamics near 10 km represents a transition from within floe behavior to forces acting between floes.

This emergent property of sea ice dynamics can be observed on various types of imagery and within small-scale models (Hopkins, 1998). On aerial reconnaissance over sea ice camps, such as the Sea Ice Mechanics Initiative (SIMI) and Surface Heat Budget of the Arctic (SHEBA) Experiments, we noted many big floes (500 m to 2 km) (WMO, 1985), with interstitial ice (Overland et al., 1998). Each floe is strong and a large amount of external energy would be required to crush, buckle or crack an individual floe. From the theory of granular media, however, a scale of approximately 10 grain widths can generally be modeled without resolving each individual element (Savage, 1998). Thus, at approximately the 10 km length scale for the central Arctic Ocean, where each floe represents an individual "grain" of ~1 km, sea ice dynamics are controlled primarily by the forces between floes rather than through the strength of individual floes. Therefore, we consider this length scale as a transition level where the details of individual floes become secondary to an emergent scale of regional ice dynamics. An analog can be made to the macroscopic behavior of wet sand.

At scales larger than 10 km, a continuum approximation of the sea ice cover becomes a valid approach to model sea ice as a granular plastic material (Overland et al., 1998). This continuum approximation does not necessarily mean that the ice dynamics representation is smooth or differentiable. The equations can be hyperbolic (Prichard, 1988), allowing for discontinuous behavior of the motion field, represented mathematically as a discontinuity in the velocity field, often called sliplines (Overland et al., 1998) or linear kinematic features (Kwok, 2001). Physically, this discontinuity might represent a 5–10 km wide damage zone where shear actually takes place. This discontinuity can also be interpreted as a slipline on Synthetic Aperture Radar (SAR) derived ice motion vectors, which directly resolve observed discontinuities at 5–10 km (Moritz and Stern, 2001; Richter-Menge et al., 2002).

A second concept from hierarchy theory is "coherent scale". A coherent scale is a spatiotemporal scale of particular importance to the functioning of a system. A major external forcing of Arctic sea ice results from wind stress. While there is some coupling of the atmospheric forcing and sea ice deformation at all scales, the 75–300 km/3–7 d spatial and temporal scale is of particular importance, and can be considered a coherent scale for sea ice due to the close match of the ice dynamics features to the length and time scales of the atmospheric wind field (Walter and Overland, 1993). Sea ice deformation generally occurs on a mesoscales (10–300 km) and slow time scales (3–7 d), while atmospheric forcing occurs at a larger spatial scale (~600 km) and a faster temporal scale (3 d). It is only where the spatial and temporal scales overlap that significant energy can be transferred from the atmosphere to the sea ice. Figure 1 illustrates this type of coherent connection, using data taken during the winter of 1992 in the Beaufort Sea during the LEADEX Experiment (Overland et al., 1995). Figure 1 shows the spectrum of the windspeed shear as red, i.e. with little variance at time scales faster than 3 d, while the corresponding spectrum of the sea ice motion is more white, indicating much more variance at shorter timescales for sea ice than for the wind field. There is a strong connection between atmospheric forcing and sea ice deformation primarily at 3–7 d, as seen in the coherence spectrum at the bottom of Fig. 1.

Another qualitative example of the scale coupling of the wind field to ice deformation is found in field observations of internal ice stress taken during SIMI (Richter-Menge and Elder, 1998). The spatial scales of small storms, such as polar lows, and wind shifts at frontal passages are too small, and these atmospheric features move too quickly for the sea ice to develop large-scale stresses. In these cases, individual floes tend to respond simply with internal oscillations, or floe–floe bumping. A shift of an air mass is generally required to create large, internal ice stress, such as strong winds blowing from a nearly constant direction for several days with a large fetch, greater than ~300 km (Overland et al., 1998; Richter-Menge et al., 2002).

Thus, based on the definition of scales for energy transfer between atmospheric forcing and sea ice

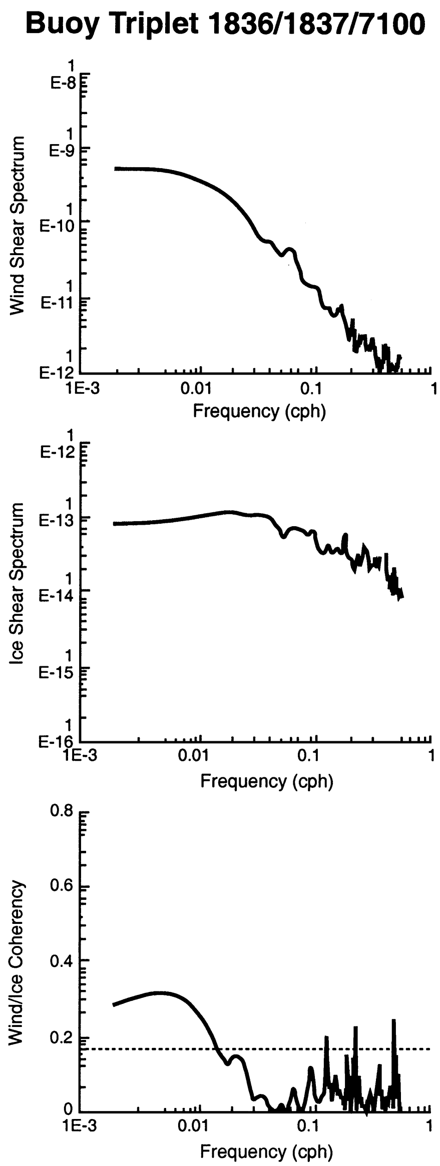


*Fig. 1.* Top: Spectrum of shearing deformation of the wind field for the central Beaufort Sea from 24 March to 24 May 1992. Units are $s^{-2}$. Data are based on anemometers mounted on buoys separated by 130 km during the Arctic Leads Experiment (LEADEX). The spectrum is red, i.e. decreases with frequency, which is typical for wind time series. Middle: Spectrum of shearing deformation in the ice field. There is much high-frequency deformation in the ice field, which is not present in the wind field. Bottom: Coherence plot between shearing deformation in the wind field and ice motion. Coherence is significant for wind forcing events longer than 3 days (after Overland et al., 1995).

deformation, we derive two important scales for Arctic sea ice: (1) an emergent property at the transition to the aggregate scale of 10–75 km and 1–3 d, and; (2) a coherent scale at 75–300 km and 3–7 d. At the coherent scale, both the spatial and temporal aspects of the atmospheric forcing and the sea ice response combine to play important roles. At scales smaller than 10 km (the multifloe and floe scales), the internal structure of the individual floes becomes important. At the aggregate (10–75 km) and coherent (75–300 km) scales, we expect considerable internal ice stress activity based on the spectrum of ice shear (Fig. 1b) in terms of hours to days. At these scales the spatial size of the sea ice aggregates plays the important role. At scales larger than the coherent scale, the time scales used to average the data are longer than those associated with direct wind forcing of sea ice dynamics, and thus we are simply temporally averaging features. Because of this averaging, we call this larger spatial and temporal domain the climatology scale, which includes two sub-divisions: the sub-basin and seasonal scales. In the remainder of the paper we further refine these scale definitions within a consistent hierarchy for sea ice dynamics.

## 2. Scale Hierarchy

Figure 2 and Table 1 illustrate and describe the classification of sea ice dynamics as defined in this study. This classification is further expanded below in terms of a hierarchical structure for sea ice dynamics based on the spatial and temporal aspects of internal and external forcing of the sea ice and the resulting deformation. Our conceptual model is not at odds with ideas of scale invariance or fractal scaling for sea ice at regional scales (Vasiliev, 1996; Korsnes, 1998). We suggest a self-similarity over the range of spatial scales larger than 10 km, based on the plastic behavior of the sea ice. We note, however, the importance of two scales for the Arctic in particular: the coherent scale, the scale of primary energy input from the atmosphere to the sea ice dynamics, and the aggregate scale, the domain of regional granular behavior of the sea ice which takes place at the transition to scales larger than the multifloe scale at ∼10 km.

### 2.1. *Floe scale*

As sea water freezes it becomes a solid. This initial freezing occurs at the subfloe, or ∼1 m scale. At the floe scale (<1 km) the dynamics are primarily due to

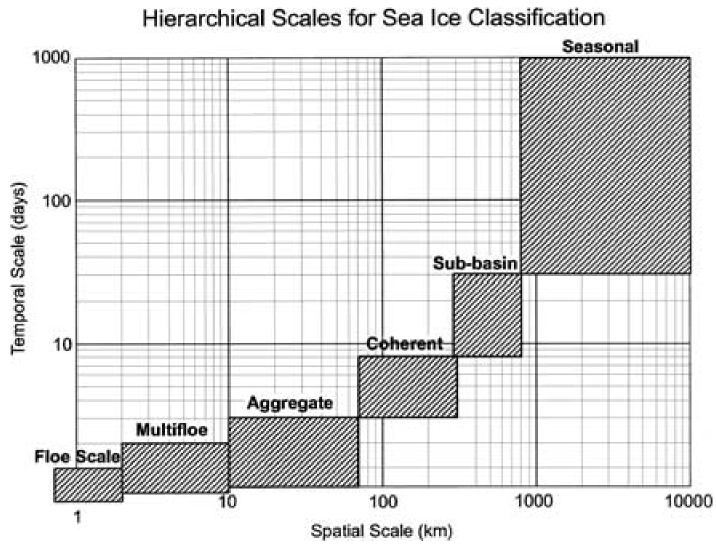


*Fig. 2.* A schematic representation of the hierarchical scales described in this article.

cracking, and take place within a floe on a timescale of less than 1 d (Demsey, 2000). Cracking relates to thermal stresses or convergence and shearing.

Figure 3 illustrates the floe scale as seen in a photo mosaic for 17 May 1998 taken during the SHEBA experiment. The image represents an area of approximately 10 km on a side. While this is a late spring image, there are still big floes (>1 km) in the region. There is an extensive linear damage zone in the upper part of the image.

Table 1. *A hierarchical classification of scales of sea ice dynamics with a description of the spatial and temporal scales of the sea ice dynamics, the matching of the atmospheric forcing to the sea ice and the associated scale of the sea ice response*

| Category | Spatial scale | Temporal scale | Wind coupling | Scale of sea ice response |
|---|---|---|---|---|
| Floe | <1 km | Hours | Too small | Within floe |
| Multi-floe | 2–10 km | 3 h–2 d | Too small | Floe-floe bumping and redistribution; ridging; |
| Aggregate | 10–75 km | 1–3 d | Too small | Differential floe motions; non-local forcing; compression wave; beginning of plastic behavior |
| Coherent | 75–300 km | 3–7 d | Best direct coupling of atmospheric scales and sea ice deformation | Motion across a field resulting in features such as arched leads, families of sliplines, and progressional compression |
| Sub-Basin | 300–700 km | 7–30 d | Matches in space, but not in time, therefore have temporal smoothing of spatial attributes | Creation of velocity “zones”; discontinuities smoothed |
| Seasonal | >700 km | >30 d | Both spatial and temporal averaging occur | Thickness fluctuations and redistribution of ice |

*Fig. 3.* A photomosaic of sea ice conditions near the SHEBA Ice Camp taken on 17 May 1998. The image represents an area of approximately 10 km on a side with big floes (>1 km) in the region, and a linear damage zone in the upper part of the image. (Courtesy Don Perovich).

### 2.2. *Multifloe scale*

At the multifloe scale (<10 km), the behavior of the sea ice is granular in nature. At this scale, statistical mechanics can characterize floe dynamics through the concept of textural and structural information taken from information theory and damage mechanics (Kerman, 1998). Direct simulation has also been completed (Hopkins, 1998). Macroscopic differences in medium response are noted whether all the grains are uniform, or have irregular shapes (Scarlett et al., 1998). We observe the multifloe scale in the correspondence between the fibrous network of cracks and ridges as seen in aircraft imagery, and under-ice thickness measurements from submarines (Kerman et al., 1999). These roughness and thickness changes derive from sea ice dynamics operating at the floe to multifloe scales (Rothrock and Thorndike, 1981; Melling and Riedel, 1995). At the multifloe scale, ridge densities and other sea ice properties can be approximated as various distribution functions, often a Poisson distribution (Lensu, 2001).

### 2.3. *The aggregate and coherent scales*

At the upper range of the multifloe scale sea ice reaches a limit where the behavior of the medium as a whole is more important than the influence of individual floes. This behavior is an emergent property, and we define this next level as the aggregate scale (10–75 km/1–3 d). At spatial scales greater than 10 km sea ice can be considered a continuum since it behaves as a plastic material, based on the interactions between floes. For example, Richter-Menge and Elder (1998) note that measured stresses in sea ice respond primarily to regional strains on the scale of 10 km. The aggregate scale includes concepts of deformation and internal stresses. At the aggregate scale, there is considerable energy in the ice motion shear spectrum (Fig. 1, center), but there is little direct atmospheric input. Here, internal stress within the sea ice has a non-local character; it is dependent on boundary conditions supplied from the next larger scale. Understanding sea ice dynamics at this level requires knowledge of the behavior of compression and shear features propagating through the sea ice, due to floes acting as a plastic medium (Hibler and Schulson, 2000).

The coherent scale (75–300 km/3–7 d) represents the next larger level in the classification, and it is key to understanding sea ice dynamics. At the coherent scale the spatial and temporal characteristics of the sea ice dynamics match the important length and time scales of the atmospheric wind field variability. This is also the scale where external boundary conditions, such as coastal geometry, are important. Both the aggregate and coherent scales consider sea ice dynamics as the response of a collection of large and small floes.

Figure 4 illustrates the differential motion of floes on the aggregate scale (inset), and the behavior of the field at the coherent level. A pair of satellite RADARSAT SAR images obtained on 5–7 December 1997 covers an area of roughly 400 km wide along the swath. The vectors show the motion of the sea ice in the vicinity of the SHEBA Ice Camp, annotated as a star, southward to the Alaska coastline. These ice motion vectors derive from a well established technique used to generate sea ice velocities within sequential SAR images (Kwok et al., 1990; Hirose et al., 1992). The large plot represents the translation of the sea ice as a field at 10 km resolution during northerly winds, and illustrates features such as arched leads and families of sliplines. Note the discontinuity in the motion (or slipline) field running north/south just to the east of the SHEBA Camp. Two other sliplines near the top of the figure and the top portion of the lower sector near $x = 150$ run more parallel to the Alaskan coast.

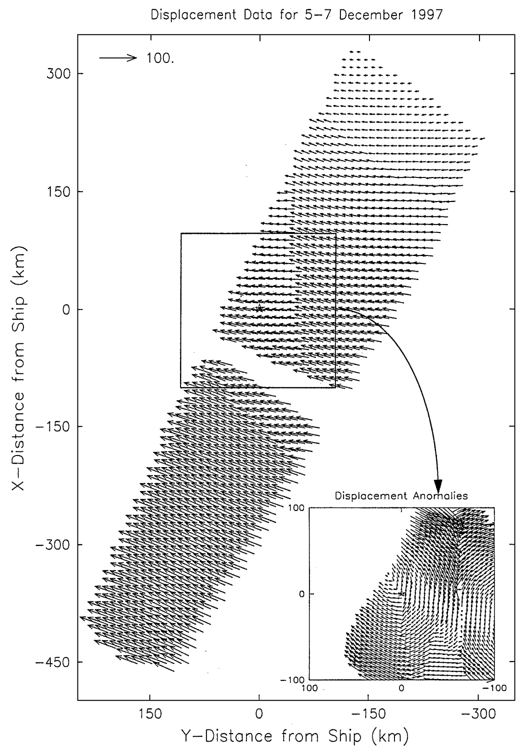


*Fig. 4.* Sea ice displacement vectors for 5–7 December 1997 derived from SAR imagery. The region is north of Barrow, Alaska and centered on the SHEBA ship (star). The resolution is 10 km and three sliplines are visible. The inset shows displacement anomalies at a 5-km resolution. Note sliplines.

These data illustrate sea ice dynamics at the coherent scale.

Figure 4 (inset) shows displacement anomalies around the SHEBA Camp at 5 km grid spacing, with the measured translation motion of the camp removed, leaving the relative motion of the ice. This differential motion observed in the field represents the aggregate scale. Here we see shearing, convergence and rotation, all representative of relative motion within the sea ice. There is considerable slipline behavior even though there is little atmospheric variability with such short length scales. The behavior is non-local in the sense that the motion is conditioned by wind stress and boundary conditions from larger spatial scales. This is also seen in the propagation of stress features within the ice field (Richter-Menge et al., 2002).

### 2.4. *The climatological scales: sub-basin and seasonal*

At the climatological scale we consider two subscales: the sub-basin (7–30 d/300–700 km) and seasonal (>30 d/>700 km). Here the spatial and temporal scales are larger and longer than the those represented by sea ice dynamics forced directly by the atmospheric wind fields, as noted in the coherent scale. Thus, we associate the spatial and temporal scales with the climatological record, i.e., statistical representations of the ice dynamics processes. At these climatological scales, the temporal averaging has an important influence on smoothing the sea ice dynamics. The modeled ice dynamics at this scale will also be smoothed, suggesting a viscous plastic formulation (Hibler, 1977; Steele et al., 1997), where discontinuities such as sliplines are smoothed within the field of motion.

Figure 5 shows sub-basin scale ice dynamics from two different sets of observations. On the bottom is a plot of the western Arctic Ocean derived from RGPS sea ice motion vectors. The bottom right figure depicts measured convergence (blue) and divergence (red), and the bottom left figure shows the associated shear (red) for 15–18 February 1998, a three day average. Areas of no change appear yellow in both images. The top figure shows sea ice conditions for 18 February 1998. The image is a Hue Light Saturation (HLS) composite of Thermal Infrared (TIR) data from the Advanced Very High Resolution Radiometer (AVHRR) combined with a swath of RADARSAT SAR data in the grey scale. The location of the SHEBA Camp is annotated in red. The color in the HLS image relates to surface temperatures of −8 °C (red) to −40 °C (blue). Compare this with the data from the RGPS convergence/divergence and shear for the 3-d period. Note the large shear line east of Wrangel Island seen at the sub-basin scale. This feature opened rapidly over hundreds of kilometers, but resulted from prolonged compaction of the sea ice against the Siberian coast (Richter-Menge et al., 2002). These data show a larger regional view of the type of events described in Fig. 4, but details at the aggregate scale are not evident.

Observations of sea ice dynamic behavior at the sub-basin scale involve statistical averaging, and the ice is often characterized in terms of its velocity zones (Maslanik et al., 1997; Miles and Barry, 1998), large-scale domains (Agnew et al., 1997) and the relationship between the Seasonal Ice Zone (SIZ) and the

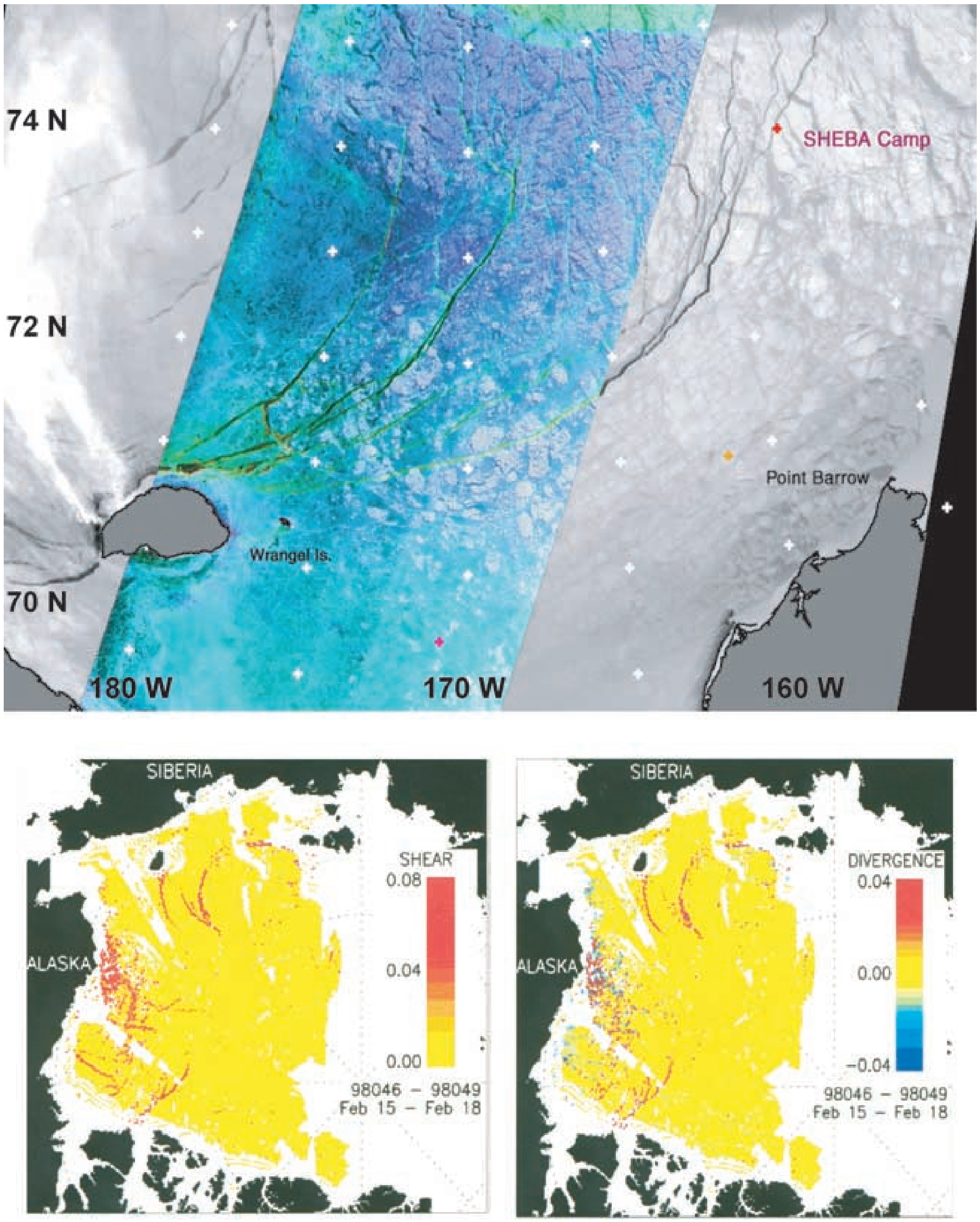


*Fig. 5.* HLS composite (left) of AVHRR TIR data (color) co-registered with a RADARSAT SAR image for February 1998. The SHEBA Camp is indicated by a red cross. Note the large deformation feature reaching from Wrangel Island near the Siberian Coast to the SHEBA Camp. The HLS composite (top) shows ice conditions for 18 February 1998. The bottom shows RGPS SAR-derived sea ice behavior averaged over the period 15–18 February 1998, at the sub-basin scale. Note the deformation features in the convergence/divergence (bottom, right) and shear (bottom, left). Also note that the bottom figures are oriented with a 90° rotation relative to the top figure.

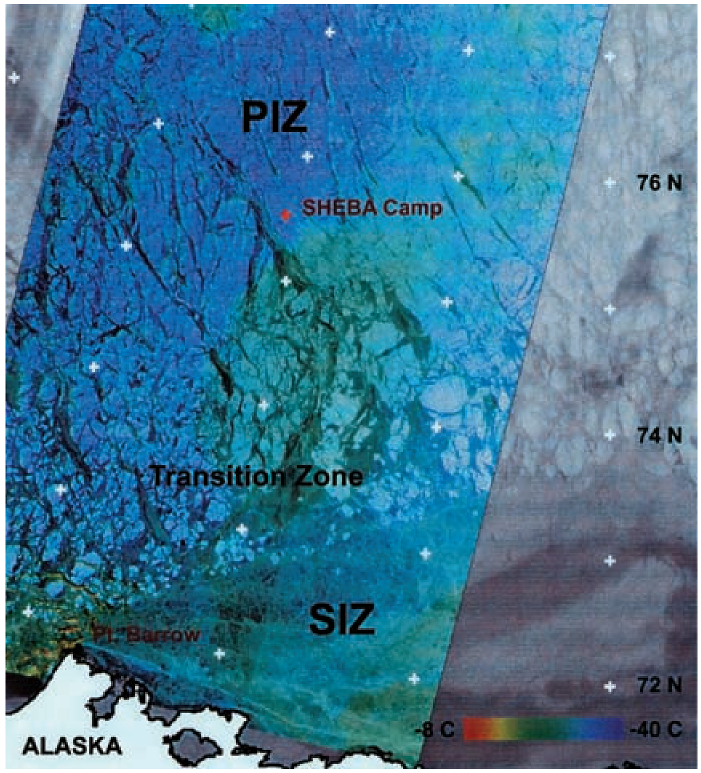


*Fig. 6.* An HLS composite of AVHRR TIR data (color) co-registered with a SAR image for 17 January 1998. Barrow, Alaska is to the south and the position of the SHEBA Ice Camp is indicated by a red cross. Note the structural differences between first year ice noted as the Seasonal Ice Zone (SIZ), the Perennial Ice Zone (PIZ), and a Transition Zone.

Perennial Ice Zone (PIZ) (Kwok et al., 1999). At the seasonal scale, variance of the combined mean observations over several years provides insight into key climatological variables, such as the interaction of the PIZ and SIZ. Figure 6 illustrates the difference in the sea ice found in the SIZ, PIZ, and a transition zone of mixed ice types. In this HLS image, taken on 17 January 1998, the multiyear ice of the PIZ appears colder (blue) than the first-year ice in the SIZ (green). The SAR texture of the SIZ in the bottom of the screen is also smoother, indicating less deformed, thinner, firstyear ice. Since we did not perform a cloud removal of any kind on the AVHRR imagery, some warmer, green areas appear in the boundary between the PIZ and the SIZ, likely due to ice smoke. The SHEBA Ice Camp is denoted by a red "+" on the image, near the PIZ boundary. The deformed nature of the sea ice in the Transition Zone ($\sim$200 km wide) indicates that it is the location of a "breccia" containing new ice within a multiyear ice matrix. Inspection of many SAR motion plots indicates that this region is highly active both dynamically and thermodynamically.

The seasonal scale ($>$30 d/$>$700 km) represents averaged sea ice characteristics based on fluctuations, extents and variability (Parkinson et al., 1999). These can include observations such as monthly averaged mean motions for a single year, or combined statistics over several years or decades. Here the temporal sampling of the data is especially important. For example, the PIZ and SIZ occur annually, but their actual extent and location vary based on different climatological conditions. Figure 7 shows the variance in sea ice motions for the month of February from seven seasons of AVHRR data and International Arctic Buoy Observations (source: J. Maslanik, University of Colorado). Note that the transition between the PIZ and SIZ off the Alaska coast appears as a discontinuity, and that the PIZ itself seems to have a rotational component of motion different from the SIZ. This rotational

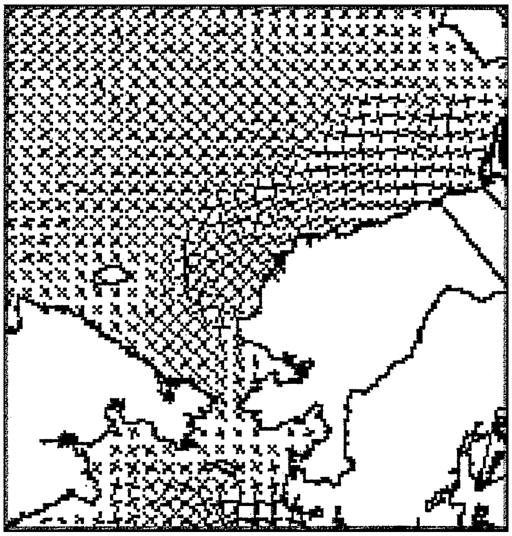

*Fig. 7.* Major and minor axes of monthly ice velocity variability for seven Februaries, 1988–1994, derived from AVHRR data. The region is the Chukchi and Beaufort Seas north of Alaska. The spacing between data points is approximately 60 km. Note the discontinuity associated with the boundary between the SIZ and PIZ. This multiyear, averaged data set represents the seasonal scale. (Figure provided by J. Maslanik, University of Colorado/CCAR.)

component of motion also appears in SAR-derived winter seasonal averages for the SHEBA period in RGPS data (Kwok, 2001).

## 3. Implications for modeling

A precursor to discussing and modeling sea ice behavior is to specify the scale of interest, and thus the processes and elements of importance. We have noted a hierarchical system of: floe, multifloe, aggregate, coherent, sub-basin and seasonal scales. Effective understanding at any particular scale (level $n$) involves defining the mechanistic behavior of the elements at the next smaller scale (level $n-1$) and considering the boundary conditions from the next larger scale (level $n+1$). Incorporating physics from the $n-1$ level usually involves parameterization, i.e., the net implication of averaging over a number of subscale events. We propose that the coherent level (75–300 km/3–7 d) constitutes the most important scale for modeling sea ice dynamics. This means that information from the aggregate scale is necessary to resolve sea ice dynamics at the coherent scale, which in turn provides the basis for calculation of the sub-basin scale. This also applies to strategies used to obtain observational data for model initialization and validation.

It is not clear that the simulation of plastic flow in isotropic viscous plastic models fully resolves the sea ice physics at the aggregate scale. It should be noted that viscous plastic models with isotropic sea ice formulations can generate long, linear features when the model is run at a high resolution ($\Delta x \sim 20$ km) (see figure from Zhang in Overland and Ukita, 2000). These features are also present with the Naval Postgraduate School model (Maslowski, personal communication). This type of long, linear feature results from the plastic nature of the model formulation, when the sea ice interacts with boundary conditions and external forcing. Though such models generate large-scale linear features, they do not seem to resolve the smaller-scale features as seen in the RGPS plots in Figs. 4 and 5. Also, the magnitudes of the modeled discontinuities appear smaller and have a larger spatial scale than those observed directly by SAR data. Perhaps the viscous formulation is a limitation, or sea ice feature orientation may play a role at the aggregate scale.

At this time of writing it is clear that the spatial resolution of sea ice models is reaching the appropriate aggregate scale, but it is unclear whether the internal ice stress term currently employed implies too much smoothing of the plastic character of sea ice at this scale. Using a Coulomb rather than an ellipse failure criterion, and resolving the thickness distribution may be important steps to applying plastic models to the aggregate scale (Overland and Ukita, 2000).

For modeling at the sub-basin scale, it is important to resolve the coherent scale. At the sub-basin scale the current generation of viscous plastic models appears appropriate (Hibler, 1979; Holland et al., 2001). However, it is important to note that increasing the resolution of the spatial and temporal calculations used in these models may not necessarily create detail consistent with observational data obtained at the aggregate scale.

## 4. Conclusions

A new classification of sea ice dynamics shows the importance of changes in sea ice dynamics from the multifloe (2–10 km) to the aggregate scale (10–75 km). The 10 km scale is important in sea ice dynamics, as this is the point at which the ice exhibits emergent behavior, providing the link between the dynamics associated with individual floes and the plastic continuum of motion based on statistical mechanics. The aggregate and coherent (75–300 km) scales both show velocity discontinuities and propagation of stress features through the ice field, demonstrating the plastic behavior of the ice cover. The coherent scale is important for modeling and observing sea ice because this is the spatiotemporal scale where ice dynamics couples most strongly with the wind forcing.

Integrity of sea ice models at all scales requires that both the model resolution and the parameterization of the sea ice physics be appropriate to the model scale. Based on SAR data and in situ observations we conclude that modeling and validating regional ice dynamics is most important at the coherent scale, which requires resolution on the aggregate scale. Modeling on the sub-basin scale must include parameterization on the coherent level, which is adequately achieved in current generation viscous plastic models. Initialization, data assimilation and validation of sea ice models requires data that correspond to the appropriate model scale, or be derived from observations taken at the next smaller scale.

## 5. Acknowledgments

We appreciate the support of ONR Arctic Programs and the NOAA Arctic Program Office. We also thank the Polar Program Office at NASA for making available the SAR data for this study. The SAR data come from the Canadian Space Agency, RADARSAT Program via the Alaska SAR Facility at UAF; the AVHRR data come from the Arctic Data Visualization and Analysis Laboratory (ADVAL), also at UAF. We thank the ASF Science Division and Ron Kwok of JPL for providing the RGPS data. Joanne Groves at ASF created the HLS composites. We appreciate the comments by the two anonymous reviewers. This is PMEL contribution 2188.

REFERENCES

Agnew, T. A., Le, H. and Hirose, T. 1997. Estimation of large-scale sea ice motion from SSM/I 85.5 GHz imagery. *Ann. Glaciol.* **25**, 305–311.

Demsey, J. P. 2000. Research trends in ice mechanics. *Int. J. Solids Struct.* **37**, 131–153.

Goldenfeld, N. and Kadanoff, L. P. 1999. Simple lessons from complexity. *Science* **284**, 87–89.

Hibler, W. D., III 1977. A viscous sea ice law as a stochastic average of plasticity. *J. Geophys. Res.* **82**, 3932–3938.

Hibler, W. D., III 1979. A dynamic thermodynamic sea ice model. *J. Phys. Oceanogr.* **9**, 815–846.

Hibler, W. D., III and Schulson, E. M. 2000. On modeling the anisotropic failure and flow of flawed sea ice. *J. Geophys. Res.* **105**, 17,105–17,120.

Hirose, T., McNutt, S. L. and Manore, M. J. 1992. Automated sea ice tracking for LIMEX '87 and '89. *Atmos. Ocean* **30**, 173–191.

Holland, M. M., Bitz, C. M. and Weaver, A. J. 2001. The influence of sea ice physics on simulations of climate change. *J. Geophys. Res.* **106**, 19,639–19,655.

Hopkins, M. 1998. In the mesoscale interaction of lead ice and floes. *J. Geophys. Res.* **101**, 21,723–21,734.

Kerman, B. 1998. A damage mechanics model for sea ice imagery. *Global Atmos. Ocean Syst.* **6**, 1–34.

Kerman, B., Wadhams, P., Davis, N. and Comiso, J. 1999. Informational equivalence between Synthetic Aperture Radar (SAR) imagery and the thickness of pack ice. *J. Geophys. Res.* **104**, 29 721–29 731.

Korsnes, R. 1998. Regime shifts in mesoscale deformations of sea ice during winter. *J. Geophys. Res.* **103**, 8167–8176.

Kwok, R. 2001. Deformation of the Arctic Ocean sea ice cover between November 1996 and April 1997: a qualitative survey. In: *Scaling laws in ice mechanics and ice dynamics* (eds. J. P. Dempsey and H. H. Shen). Kluwer Academic Publishers, Boston, 315–323.

Kwok, R., Cunningham, G. F. and Yueh, S. 1999. Area balance of the Arctic Ocean perennial ice zone. *J. Geophys. Res.* **104**, 25 747–25 759.

Kwok, R., Curlander, J. C., McConnell, R. and Pang, S. S. 1990. An ice-motion tracking system at the Alaska SAR Facility. *IEEE J. Ocean. Eng*. 44–54.

Lensu, M. 2001. A downscaling structure for distributions describing ice characteristics. In: *Scaling laws in ice mechanics and ice dynamics* (eds. J. P. Dempsey and H. H. Shen). Kluwer Academic Publishers, Boston, 449–456.

Maslanik, J., Fowler, C., Key, J., Scambos, T., Hutchinson, T. and Emery, W. 1997. AVHRR-based Polar Pathfinder products for modeling applications. *Ann. Glaciol.* **25**, 298–302.

Melling, H. and Riedel, D. A. 1995. The underside topography of sea ice over the continental shelf of the Beaufort Sea in winter 1990. *J. Geophys. Res.* **100**, 13 641–13 653.

Miles, M. W. and Barry, R. G. 1998. A 5-year satellite climatology of winter sea ice leads in the western Arctic. *J. Geophys. Res*. **103**, 21 723–21 734.

Moritz, R. E. and Stern, H. L. 2001. Relationships between geostrophic winds, ice strain rates and the piecewise rigid motions of pack ice. In: *Scaling laws in ice mechanics and* *ice dynamics* (eds. J. P. Dempsey and H. H. Shen). Kluwer Academic Publishers, Boston, 335–348.

O'Neill, R. V., DeAngelis, D. L., Wade, J. B. and Allen, T. F. H. 1986. *A hierarchical concept of ecosystems*. Princeton University Press, Princeton, NJ, 253 pp.

Overland, J. E. and Ukita, J. 2000. Dynamics of Arctic sea ice discussed at workshop. *Eos Trans. AGU* **81**, 309–314.

Overland, J. E., Walter, B. A., Curtin, T. B. and Turet, P. 1995. Hierarchy and sea ice mechanics: A case study from the Beaufort Sea. *J. Geophys. Res.* **100**, 4559–4572.

Overland, J. E., McNutt, S. L., Salo, S., Groves, J. and Li, S. 1998. Arctic sea ice as a granular plastic. *J. Geophys. Res.* **103**, 21 845–21 868.

Parkinson, C. L., Cavalieri, D. J., Gloerson, P., Zwally, H. J. and Comiso, J. C. 1999. Arctic sea ice extents, areas and trends, 1978–1996. *J. Geophys. Res.* **104**, 20 837–20 856.

Prichard, R. S. 1988. Mathematical characteristics of sea ice dynamics models. *J. Geophys. Res.* **93**, 15 609–15 618.

Richter-Menge, J. A. and Elder, B. C. 1998. Characteristics of pack ice stress in the Alaskan Beaufort Sea. *J. Geophys. Res.* **103**, 21 817–21 829.

Richter-Menge, J. A., McNutt, S. L., Overland, J. E. and Kwok, R. 2002. Relating Arctic pack ice stress and deformation under winter conditions. *J. Geophys. Res.* **107**, 8040.

Rothrock, D. A. and Thorndike, A. J. 1981. Geometric properties of the underside of sea ice. *J. Geophys. Res.* **85**, 3955–3963.

Sanderson, T. J. O. 1988. *Ice mechanics: risks to offshore structures.* Graham and Trotman, London.

Savage, S.B. 1998. Analysis of slow high-concentration flows of granular materials. *J. Fluid Mech.* **377**, 1–26.

Scarlett, B. M. van der Kraan, and Janssen, R. J. M. 1998. Porosity: a parameter with no direction. *Philos. Trans. R. Soc. London* **356**, 2623–2648.

Steele, M., Zhang, J., Rothrock, D. and Stern, H. 1997. The force balance of sea ice in a numerical model of the Arctic Ocean. *J. Geophys. Res.* **102**, 21 061–21 079.

Vasiliev, L. 1996. Fractals in sea ice and properties of its multiscale images. In: *Progress in environmental remote sensing research and applications* (ed. E. Parlow). Rotterdam, NED, 241–248.

Walter, B. A. and Overland, J. E. 1993. The response of lead patterns in the Beaufort Sea to storm-scale wind forcing. *Ann. Glaciol.* **17**, 219–226.

WMO, 1985. "Sea Ice Nomenclature", Supplement No. 4, World Meteorological Organization, WMO/OMM?BMO-No. 259, TP. 145.

Zhang, J., Rothrock, D. and Steele, M. 2000. Recent changes in Arctic sea ice: The interplay between ice dynamics and thermodynamics. *J. Climate* **13**, 3099–3114.